



Determination of a process window with consideration of effective layer thickness in SLM process

Il Hyuk Ahn^{1,2}

Received: 3 September 2018 / Accepted: 6 September 2019 / Published online: 28 October 2019
© Springer-Verlag London Ltd., part of Springer Nature 2019

Abstract

Selective laser melting (SLM) process based on metallic powders has been broadly adopted for its higher accuracy. In the SLM process, the building of a process window is a fundamental work for fabricating a full-dense part for a new material. Single-track test (STT) has been widely used due to its simplicity. Due to the different environmental conditions of between STTs and a real fabrication, stable process parameters obtained from the STTs cannot ensure successful fabrication. To resolve the problem, this paper proposes a new method to build a process window based on multi-layered fabrication. From the comparison between existing and proposed method, it is concluded that the proposed method can stably build a process window for a hard-processed material and provide more information for a geometrically accurate fabrication and the surface quality of a fabricated part.

Keywords Additive manufacturing · Effective layer thickness · Multi-layered single-line track test · Process window · Selective laser melting · Single-track test

1 Introduction

Selective laser melting (SLM) process is a promising additive manufacturing technology based on the fusion of the metallic powders with layer-by-layer manner. Due to its three-dimensional accuracy, the SLM process has been broadly adopted in various fields such as aerospace, defense, medical, and vehicle manufacturing [1–4]. Especially, the aerospace field utilizes the SLM process to make parts with high-performance using hard-machined materials [5–7]. In the SLM process, the spherical metal powders on a working bed are melted by selectively high-power laser scanning, and the metallic powders melted by the laser are fused onto a previous layer or substrate. The process is continued until the top layer is finished, resulting in a completed 3D part [8–10]. For the fabrication of the 3D part, the laser scan path can be generated by special software. In the generation of the laser scan path, three different laser scan modes are employed to fabricate a

full-dense 3D part. These modes are contour, fill, and fill-contour scan modes [11, 12]. Each scan mode has a number of parameters to be optimized. For example, contour-scan mode needs two parameters (laser power W , and scan speed mm/s), while hatch space (mm) is additionally needed for the fill-scan mode. The scan modes have different roles. Contour-scan mode is used to form a contour curve of a fabricated part. Thus, the surface quality of the fabricated part is dependent on the parameters of contour-scan mode. Fill-scan mode is used to fill an area within the contour curve of a fabricated part. To fill the inner area of the part, hatch space, defined as the distance between two neighboring scan lines, should be added as another process parameter. The fill-contour-scan mode is used to form lines parallel to the contour-scan lines to join fill-scan lines with contour-scan lines. Two process parameters are enough to form a fill-contour-scan line. As mentioned above, in the SLM process, all laser scan modes are based on a scan line. Thus, the stability of an individual scan line for the SLM process can be secured. To guarantee the stability, the process parameters for a stable scan line should be properly selected [13, 14]. To determine the optimal values for the parameters including laser power and scan speed, single-track test (STT) based on a scan line has been widely adopted due to its simplicity.

Di et al. performed single-track experiments and the tracks obtained were classified into four different types: regular-

✉ Il Hyuk Ahn
ahnih@tu.ac.kr

¹ School of Mechanical Engineering, Tongmyong University, Busan 48520, South Korea

² Center for Mechanical Convergence Engineering, Busan 48520, South Korea

thick, regular-thin, regular-broken, and irregular-pre-balling types [15]. Based on the results of the single-track experiments, they concluded that the regular-thin track condition was most favorable for the fabrication of a 3-D part using the SLM process with the consideration of both productivity and process stability. Laser melting conditions can be classified in various ways, depending on the type of material. Zhang et al. reported a process window for W-Ni-Cu alloy with four track types: no-melting, slightly melting, spheroidization, and appropriate melting [16]. Song et al. generated process windows over the ranges of laser power (60, 80, and 100 W) and scan speed (0.2–1.4 m/s) with MH300 (hydrogen-reduced sponge iron) metal powders [17]. The generated process windows were divided into four zones: deformation zone, formation zone, the zone of the poor formation, and zone of non-forming. Li et al. defined the single-track types as over melting, moderate melting, balling, and insufficient melting for the process window of W-Cu 1:10% alloy [18]. Childs et al. showed process windows for stainless steel and tool steel with five different track types [19]. As a special case, Khan et al. reported a process window for pure gold powder with a very narrow stable zone [20]. The classification of the single-track types mentioned above was based on observing the fabricated tracks from top view. Gong et al. and Kempen et al. used the fabricated single-track shapes from cross-sectional views to determine the stability of the SLM process. This is the reason that, under the conditions of high laser power and low scan speed, a keyhole effect could appear in the bottom of a track, resulting in degraded mechanical properties [21]. The literature mentioned above has said that the generation of a process window should precede the process research on new material. However, in the real fabrication of 3D parts using the SLM process, multi-line and multi-layered tracks are used, and a layer thickness with layers is changed during the fabrication due to the powder packing density [22]. Thus, the condition for STTs is different from the condition of the real fabrication. Specifically, the changed layer thickness becomes more critical in the fabrication of a part with thin/small features/supports or hard-processed material. In tests for generating the process window, the change of the layer thickness should be considered to guarantee the formation of a stable track throughout fabrication.

To address this problem, this paper proposes a new method to determine a stable process window for the SLM process and discusses the advantages of the proposed method. Based on the multi-layered single-line tracks, the proposed method can evaluate the stability of the SLM process with considerations of the unfavorable phenomena and an effective layer thickness changed with layers as well. In addition, the specimens formed for the proposed method can serve the lateral surface roughness and the width of a single scan track. The measured lateral surface roughness can be used to select the candidates of the optimal process parameters for the contour-scan mode.

The width of a scan line can be utilized to determine a parameter value, named beam compensation, which influences the geometric accuracy of a fabricated part. As mentioned above, the proposed method has additional advantages, comparing to the existing method. The details of the proposed method will be explained in next sections. The material used and the fabrications of the specimen will be described in Section 3. Section 4 will analyze the measured results and discuss the results. In Section 5, conclusions will be drawn.

2 Proposed method

2.1 Stability of SLM process

Laser power and laser scan speed are main parameters in a typical single-track test (STT) which is used to evaluate the stability of the SLM process. In the STT, the ranges of the laser power and the laser scan speed are depended on the specifications of an SLM machine. In general, the STT is performed with the two parameters under the equal-interval condition. To estimate the stability of the scan tracks, two aspects should be considered as the continuity of the scan tracks from the top view and the sectional shape of the scan tracks. From the top view, the continuity of the scan tracks is firstly evaluated due to the easiness of the evaluation. In the continuity evaluation from the top view, the formation of regularly and frequently broken tracks and balling phenomenon can be observed, which deteriorates the stability of the powder deposition condition in a subsequent layer [23]. However, the image from the top view cannot explain the inner condition of the scan tracks. To estimate the inner condition, sectional images should be secondly evaluated. From the sectional images, the penetrated depth of melt pool and keyhole geometry can be identified. To assure the fusion of two successive layers, the penetrated depth of the melt pool should be comparable to the predetermined layer thickness. The keyhole geometry should be evaded to avoid the deterioration of properties of a fabricated part. As aforementioned, the stability of the scan tracks has been evaluated by the two aspects. However, the method cannot guarantee the stability of laser scanning for multi-line and multi-layered tracks.

2.2 Multi-layered single-line track test method

Until now, the STT method has been widely adopted to build a process window for the SLM process. However, multi-line and multi-layered tracks have been used to fill a volume. Thus, the stable condition obtained from the STT method would be unstable in the fill-scan mode due to the different environment in powder deposition. Thus, a new method should consider the difference. In this paper, the proposed method is based on the multi-layered tracks and the specific

scanning patterns. The powder deposition condition for the fabrication of specimens is close to the condition of the fill-scan mode. Hence, the proposed method can build a more reasonable process window than STT method. Figure 1 shows the schematic diagram of the proposed method.

In the proposed method, the scan pattern can be characterized by parallel scan lines. To realize the parallel scan lines, this paper uses a wide hatch space (mm) that is defined as the distance between neighboring two scan lines. When the large hatch space is used, neighboring two scans have no overlap, resulting in forming independent scanned lines. In this paper, the value of the hatch space was used as 0.7 mm [12]. The scan pattern was sustained from bottom to top layers. As shown in Fig. 1, the proposed method can be characterized by multi-layered single-line tracks, which fabricates specimens under the similar condition of the fill-scan mode. So, hereafter, the proposed method would be called as MLSTT (multi-layered single-line track test) method.

3 Experiments

3.1 Equipment and materials

In this work, a ProX300 (3D Systems, USA) machine was used to fabricate the specimens. The machine has a 500 W ytterbium fiber laser with a spot size of 75 μm diameter and a wavelength of 1070 nm. During fabrication, a working chamber in the machine was filled with nitrogen gas to prevent oxidation of fabricated specimens. The inert gas was circulated by a vacuum pump to remove fumes or by-products produced during laser scanning. After the laser scanning process for a layer was finished, the working platform moved down a distance equal to a layer thickness (20 μm). A cylindrical recoater in the powder deposition system spread powders on the working bed. This routine was continued until the top layer of a part was completed.

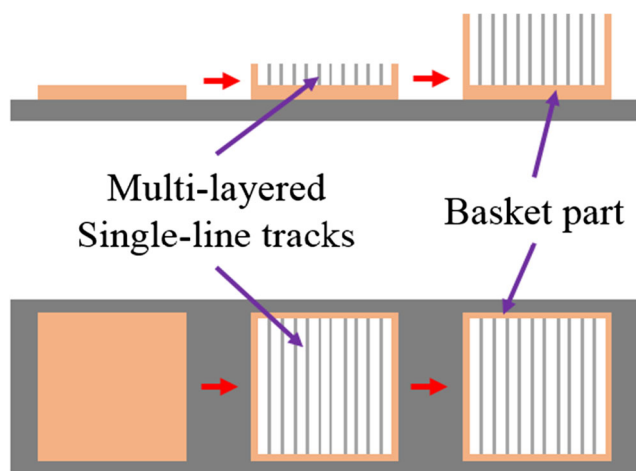


Fig. 1 Schematic diagram for the proposed approach

In the SLM process, stainless steel powders (stainless steel, STS630) were used to produce specimens. The chemical composition and SEM morphology of STS630 powders (FE-SEM with EDS, FEI) are shown in Table 1 and Fig. 2, respectively. The distribution of powder particles (laser scattering particle size analyzer, LA-950, HORIBA) is shown in Fig. 3. Fabricated specimens were cut using a wire EDM machine and mounted to take cross-sectional images with an optical microscope (GX51, OLYMPUS). After polishing, the mounted specimens were etched with Waterless Kalling's reagent (5 g CuCl_2 + 100 cc ethyl alcohol) to characterize their microstructure.

3.2 Fabrication of specimens

Because the STTs are based on a single-line scan of a laser, the STTs only need a powder deposition process (20 μm thickness) and a laser scans over the deposited powders with different laser powers and scan speeds. In this paper, laser powers in the range of 120–420 W and laser scan speeds in the range of 100–4000 mm/s were used, and the length of each scan line was 10 mm.

In the specimen fabrications, laser powers and scan speeds are still variables to be controlled. The same range and interval for the two parameters were used for the comparison. As shown in Fig. 1, specimens for MLSTTs consist of two parts. One is a basket part to protect multi-layered single-line tracks when the specimens are cut from the substrate. Another is a main part to examine the stability of the process with parameters. In the fabrication of the basket part, the process parameters were determined based on the process parameters of 316 L material [24]. While, in the fabrication of the main part, two process parameters such as laser power and scan speed were varied. After the fabrications of specimens with the various conditions, all specimens were cut from the substrate. The specimens were evaluated for the process stability with the combinations of process parameters. After investigating the stability with process parameters, successfully fabricated specimens were cut orthogonal to the fill-scan direction to obtain additional information.

4 Results and discussion

4.1 Results from STTs

In the aforementioned section, single-track tests (STTs) were performed. To evaluate the stability of the single-line tracks

Table 1 Chemical composition of STS 630

Element	Fe	Si	Cr	Mn	Ni	Cu
Wt%	Balance	0.68	16.36	1.2	4.56	4.83

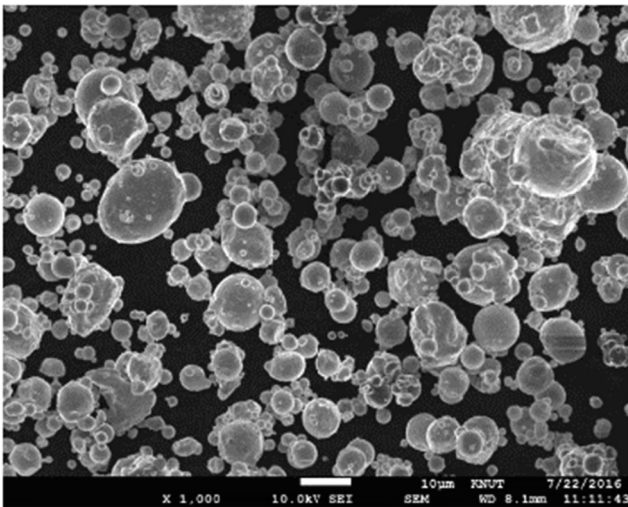


Fig. 2 A SEM morphology of STS 630 powders

with various conditions, images from the top and the section views of each single-line track were taken. Table 2 shows the images from the top view in laser power of 170 W. In lower scan speeds such as 100–200 mm/s, track widths are larger than the widths of tracks in other scan speeds and looks like continuous scan tracks. In the range of 300 to 500 mm/s, track widths gradually are decreased with scan speeds and still continuous scan tracks are observed. Whereas, irregular scan tracks and broken tracks can be observed over 1200 mm/s. It would be said that stable conditions in a laser power of 170 W were the range of 100 to 1000 mm/s, in the viewpoint of the continuity of scan tracks from the top view, while the images from the section view show the different stable region, compared with the stable region observed from the top view. Table 3 shows the images from the section view in 170 laser power. From Table 3, the shape of the melt pool was evaluated with scan speeds. In scan speed of 100 mm/s, some voids are observed. The voids frequently appear in higher energy density like the combination of high power and low scan speed. The phenomenon is known as the keyhole effect which should be avoided to prevent the deterioration of the mechanical properties. With the increase of the scan speed, the keyhole geometry in the melt pool is moderated and the bead shape becomes more circular. In the further higher scan speed, the shape of the melt pool becomes stable. At the scan speed of

1400 mm/s, it can be seen that the bead has a less contact area with the substrate. It means that the surface tension increases and the formation of the broken or irregular track could be observed as shown in Table 2. As mentioned in the above paragraph, to exactly determine the stable process region, the stability of the scan tracks in STTs should be evaluated with the two considerations of the continuity of the scan track from the top and the sectional shape of the melt pool from the section view.

Based on the two viewpoints, the stability for the diverse combinations of laser powers and scan speeds was evaluated as shown in Fig. 4. In Fig. 4, it can be seen that the stable region is different between the top view and the section view. In the results from the top view, the stable region is in the wide range of 120 to 320 W and of 100 to 1000 mm/s. In the range, the tracks form the continuous lines and the widths of the tracks are gradually decreased with laser scan speeds in certain laser power. However, above a certain scan speed (here, 1200 mm/s), the continuity of the tracks is disappeared and the tracks show the broken or irregular shapes, while the results from the section view show the different trend. In the range of the low scan speed (100 mm/s–1000 mm/s) estimated as the stable region from the top view, there are no stable conditions. In the relatively higher scan speed (> 1200 mm/s), the stable tracks are mainly observed.

To understand the difference between the two results, two reasons should be explained. One is powder scattering and another is keyhole effect. $D_{90\%}$ size of powders used in this paper is about 20 μm and a layer thickness is the same as the $D_{90\%}$ size of the powders. It is difficult to deposit the small size powders for the small layer thickness on the working bed but the machine can spread the small size powders using a roller type deposition system. When the powders deposited with a layer thickness of 20 μm are exposed by a higher scan speed, powders can be easily scattered. The deposition stability of the powders on the bed is rapidly deteriorated, finally leading to the irregular or broken track as shown in Fig. 5a. Thus, the stable region is limited by the laser scan speed to prevent the powder scattering, resulting in no stable region beyond a certain scan speed. However, the segment of the fused tracks could be a stable shape, depending on the position of a cutting plane as shown in Fig. 5b. The phenomenon could cause the difference between the results

Fig. 3 Distribution of powder particles for STS 630

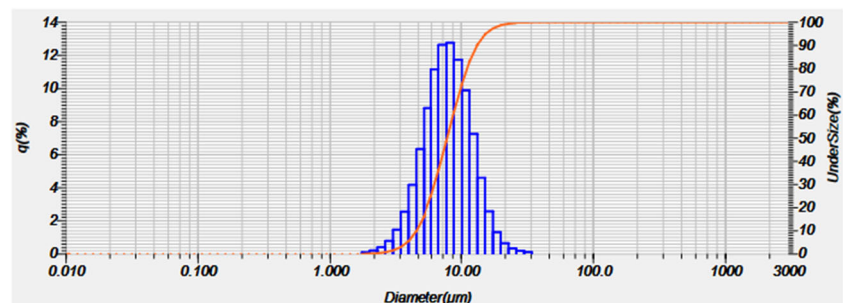

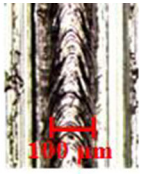

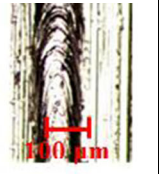




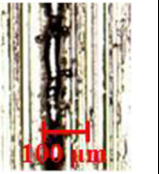



Table 2 Results from top view in 170-W laser power

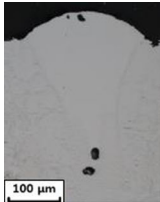
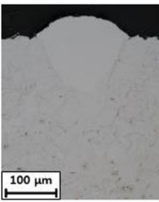
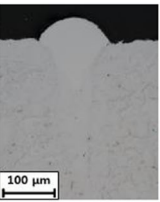
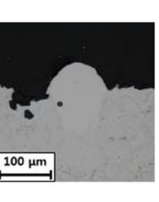
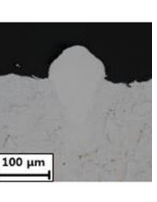
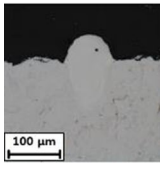
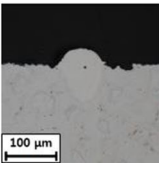
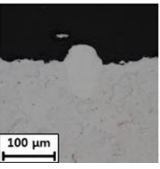
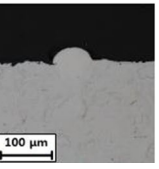
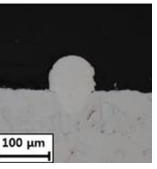
		Scan speed (mm/s)				
		100	200	300	400	500
Images from top view						
		600	800	1000	1200	1400
						

from the top and the section views. Another reason to cause the difference is the keyhole effect [21]. The keyhole effect widely observed in welding process appears at a lower scan speed and a high laser power in the SLM process. The keyhole cannot be identified from the top view but can be only observed from the section view. Thus, as shown in Tables 2 and 3, even though the stable region from the top view is identified, the region could be finally estimated as the unstable region due to the keyhole phenomenon. As stated above, it is hard to determine the stable process window and an amount of experience is needed to exactly evaluate it because the two results of the top and the section views from STTs could be different. It causes the development of a new method to estimate the stability of the SLM process.

4.2 Multi-layered single-track tests

In this paper, to demonstrate the effectiveness of the proposed method, specimen fabrications based on parallel scan lines were conducted as shown in Fig. 1. During the fabrication process, unstable fabrications were stopped to maintain process stability. Table 4 shows images from the top view in a laser power of 170 W. Although diverse scan speeds in a laser power of 170 W were employed in the specimen fabrications, successful fabrications only were performed over a certain condition like 1000 mm/s at 170 W. With increasing the scan speed, the condition of the formed tracks becomes unstable, and in a severe case, the broken tracks are observed. It can be

Table 3 Results from sectional view in 170-W laser power

		Scan speed (mm/s)				
		100	200	300	400	500
Images from sectional view						
		600	800	1000	1200	1400
						

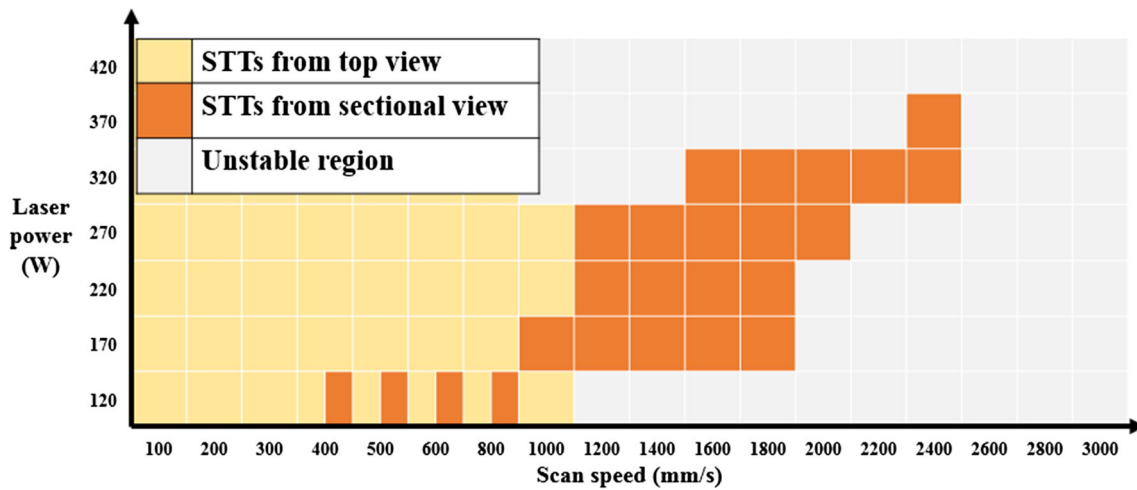


Fig. 4 Stability comparison between results from top and section views

understood that the reduction of the track width in lower layers with scan speeds aggravates the stability of the powder deposition process, finally leading to increasing the process instability. Figure 6 shows the influence of the reduction of the track widths for the process stability. In Fig. 6a with a narrow width in lower layers, segments with the narrow width are observed. While in Fig. 6b, the track width increases with height and the width become stable over a certain height. The variation of the track width with layers influences the straightness of the formed track as shown in insets of Fig. 6. Thus, it can be said that the straightness of the formed tracks from the top view becomes an important factor. Based on the straightness, the process stability with the process parameters was evaluated and summarized in Fig. 7. In the evaluation of the stability in the multi-layered single-track tests (MLSTTs), there is no mathematical formulation. However, the straightness of the formed track is steeply changed in the boundary between stable and unstable conditions and the determination of the stable process parameters can be easily performed due to the steep change. In the boundary region, the determination could be affected by the experience of the evaluator for the process stability. But, it is no easy to use the boundary condition as the optimal process parameters for the quality of a part. Thus, the estimation of the main region is more important. The

stable region from MLSTTs as shown in Fig. 7 is similar to the stable region from the section view. It means that MLSTTs can firmly estimate the stability of the process with process parameters.

4.3 Comparison between STTs and MLSTTs

In the previous section, results from two methods, STTs and MLSTTs, were explained. Figure 8 shows the comparison of results from the two methods. In Fig. 8, two facts can be obtained. One is the stable regions obtained from the two methods is overlapped, which shows that MLSTTs can evaluate the process stability with the combination of two process parameters. Another is that stable scan speeds in MLSTTs are faster than stable scan speeds in STTs at the same laser power in no overlapped region between two methods. It can be explained by the comparison of the stability of powder deposition in between the first layer and a higher layer. Powders deposited on the fine surface of the working plate could be easily scattered by a higher scan speed of laser, resulting in the formation of the unstable tracks, while powders in a higher layer are deposited on powders or scanned tracks and the powder scattering by laser scanning is restricted by the surround powders. The deposited powders stably stay during

Fig. 5 Images from the top and section views in a laser power of 220 W and a scan speed of 1600 mm/s

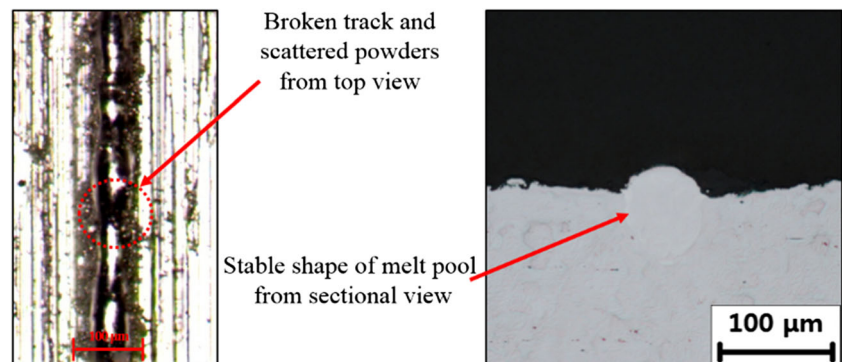


Table 4 Results of MLSTTs from the top view in a laser power of 170 W

Images from the top view	Scan speed (mm/s)					
	1000	1200	1400	1600	1800	2000
	2200	2400	2600	2800	3000	3200

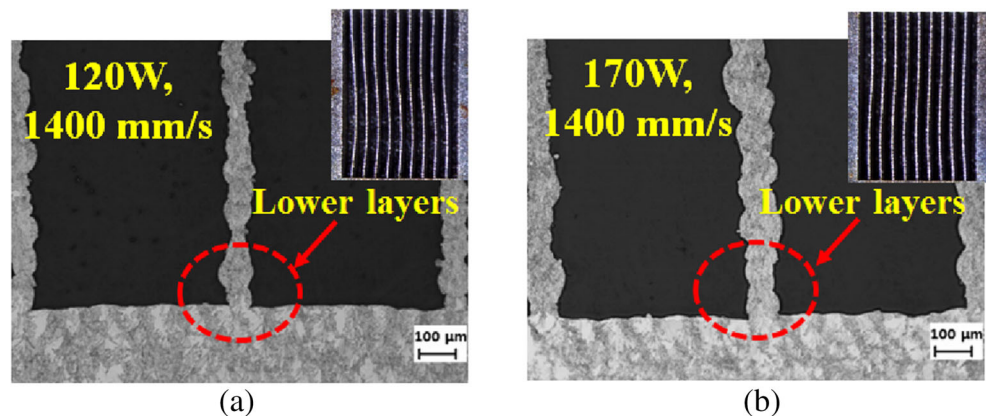
laser scanning with the higher speed, and the stable tracks could be formed. It seems that stable scan speeds in MLSTTs are faster than stable scan speeds in STTs. Although a little difference between the two methods, it can be said that MLSTTs can estimate the process stability with ease and accuracy.

4.4 Discussion

In the SLM process, there are two kinds of layer thickness such as nominal and effective layer thickness. The nominal layer thickness is a predetermined thickness before the fabrication and this thickness is not changed during the fabrication. While effective layer thickness is changed with layers. After a certain layer, the effective layer thickness converges on a specific value. To explain the change of the effective layer thickness, packing density of materials and shrinkage should be considered. Because the spherical metallic powders are used for the SLM process, a volume filled with the powders has a

lot of voids. The percentage of the voids for the volume can be changed with the size distribution of powders, which is called as the packing density of powders. According to the packing density, a powder deposition thickness is varied. Spierings et al. reported the change of the effective layer thickness with the packing density and a nominal thickness as shown in Fig. 9 [22]. As shown in Fig. 9, in the first layer, the layer thickness is the same as the nominal layer thickness, but the effective layer thickness increases until 8~10 layers. After 10 layers, the effective layer thickness becomes stable to a certain value. They explained the phenomena with the shrinkage in the vertical direction caused by the packing density of below 100%. It should be noted that the effective layer thickness was changed with layers. In STTs, the thickness of the deposited powders is the same as the nominal thickness. Thus, STTs can only evaluate the stability of the conditions under the nominal layer thickness. However, the effective layer thickness is changed with layers, and the stability could be different with the change. In the STTs using a nominal layer, the change of

Fig. 6 Images from the bottom of the specimens in (a) 120 W, 1400 mm/s, and (b) 170 W, 1400 mm/s. Images from the top view were inset, respectively



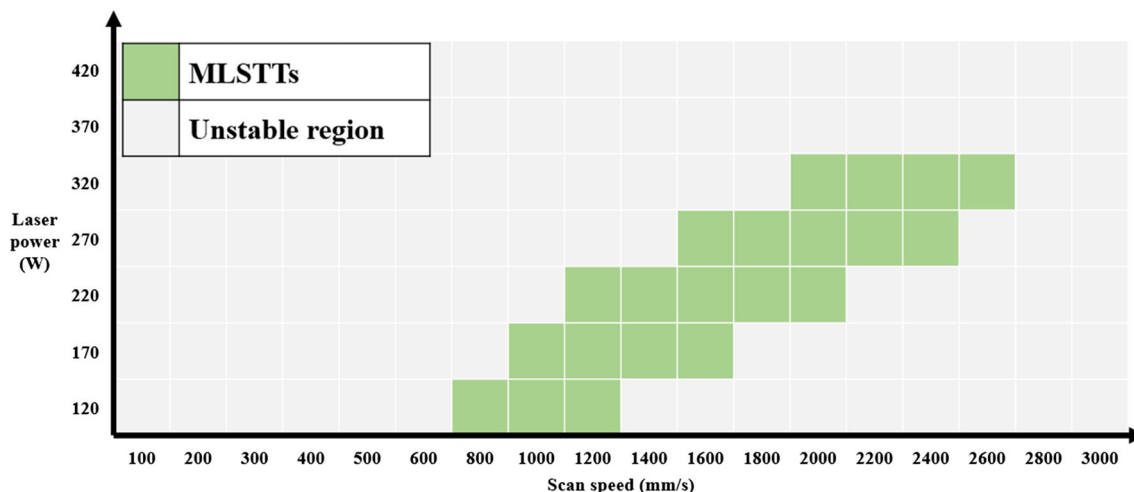


Fig. 7 Stable region obtained from MLSTTs

the effective layer thickness is not considered, while MLSTTs can evaluate the process stability with the consideration of the change of the effective layer thickness because the MLSTTs is based on the multi-layered fabrication. In addition, the consideration of the changed layer thickness is more critical in the fabrication of a part with hard-processed materials such as Ti alloy and Ni alloy with low heat transfer coefficients but with high functionality. We believed that the advantage of the proposed method can help the research of the SLM process for new high functional materials.

Addition to the advantage, MLSTTs has two other advantages. First, the width of the single-line track can be measured. In SLM processes, contour-scan establishes the contour of a part and the path of the contour-scan should be offset to compensate the width of the contour-scan for dimensional accuracy. To compensate the width of the contour-scan line, a parameter, known as beam compensation value (or beam offset), is used. The value of the parameter is generally recommended as half of the width

of the single-line track. Thus, the measurement of the width of the single-line track is important. The measurement can be implemented utilizing the proposed method. A method to measure the width of the single-line track for the contour-scan was proposed in the previous paper of author [12]. The method is very similar to the proposed method in the way that the specimen is fabricated by parallel scan lines with a large hatch space in the fill - scan. However, in the previous work, specimens with parallel scan lines were fabricated, not to build a process window, but to measure the width of the single-line track. Figure 10 shows the measured results of the width of the single-line track at 170 W of laser power. The measured widths decrease with scan speeds as other studies are reported [25, 26].

Second, it is possible to estimate the lateral surface roughness with the change of the process parameters. Specimens have a number of thin walls within a volume, due to parallel scan lines with a large hatch space. The

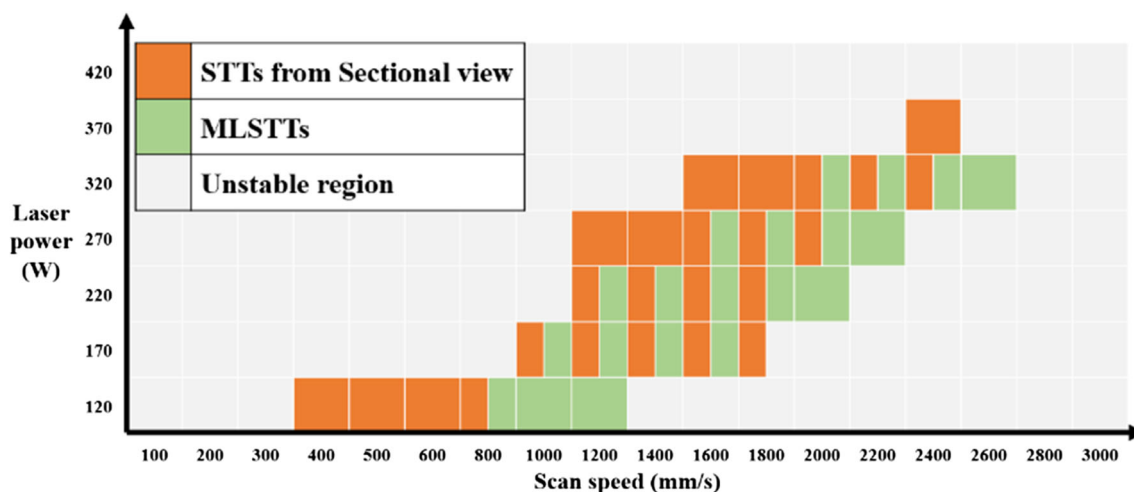
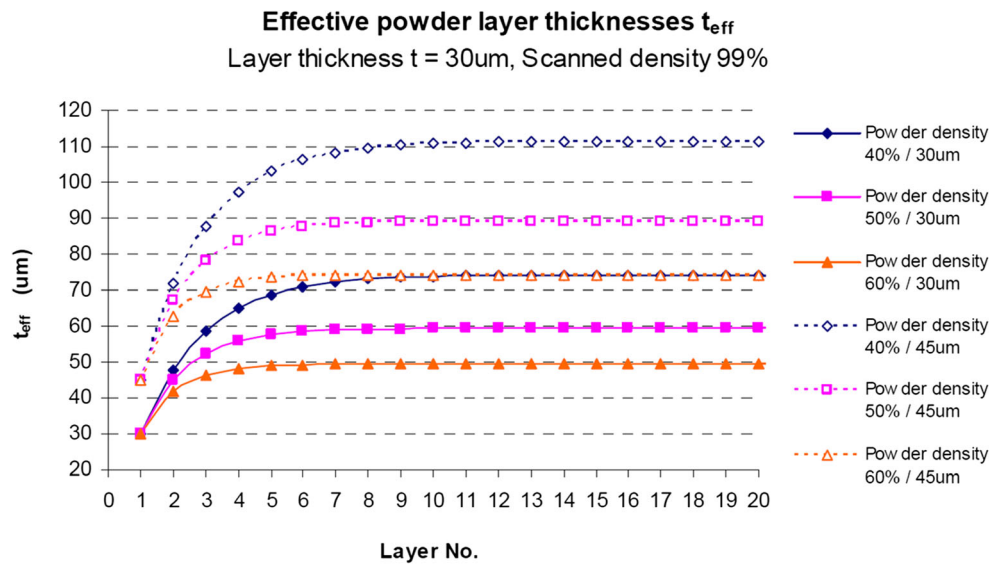


Fig. 8 Comparison of the stable process windows between STTs and MLSTTs

Fig. 9 Development of the effective layer thickness with nominal layer thickness and packing density [22]



thin wall can be understood as the lateral side wall of a part because the processing environment for the thin wall is very close to one of the contour-scan. The lateral surface roughness of the thin wall can be used to estimate the lateral surface roughness of a dense 3D part, although the surface roughness of the two does not agree exactly. Hence, the lateral surface roughness of specimens fabricated with diverse process parameters can be utilized to narrow the range of the candidates of the optimal process parameters for the contour laser scan [27, 28]. The measurements of the lateral surface roughness were performed. The measured results at 170 W of laser power are shown in Fig. 10. Figure 10 shows that the optimal scan speed in the case of 170 W of laser power is determined as 1400 mm/s of scan speed based on the lateral surface roughness (Fig. 11).

As discussed previously, the proposed method can evaluate the stable process window and provide more useful information related to the optimization of SLM process. In the SLM process with small size powders and a shallow layer thickness, the proposed method can stably estimate the process window.

5 Conclusions

In this work, a new method was proposed to build a process window for an SLM process and showed the usefulness of the proposed method using experiments. From the analysis of the experimental results, the following conclusions are drawn.

- 1) In the STTs, the analysis of images from the top and section views should be performed to build an accurate process window. From the analysis of an image from the top view, small size powders can be scattered by the laser with a high scan speed and the scattering of the powders can influence the continuity of the scan track. Thus, in the estimation of the process stability for SLM process with small size powders, images from the section view should be utilized to obtain the accurate process window. In an analysis of images from the section view, the keyhole effect should be carefully evaluated to build the process window.
- 2) The advantage of the proposed method is able to consider the change of the effective layer thickness with layers for the evaluation of the process stability. Because the

Fig. 10 Measurements of the width of the single-track lines obtained from MLSTTs

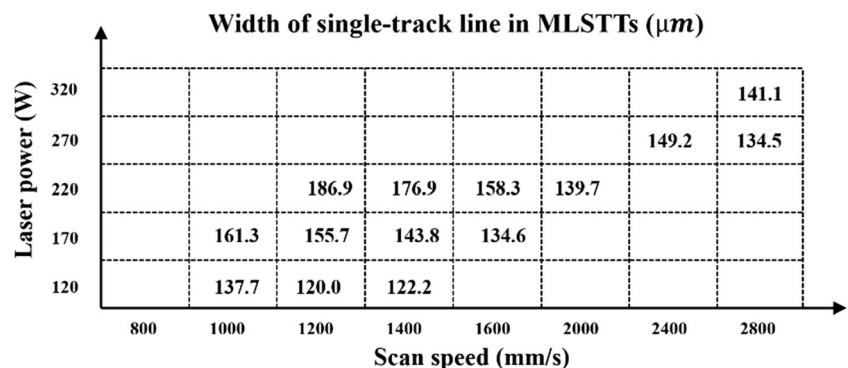
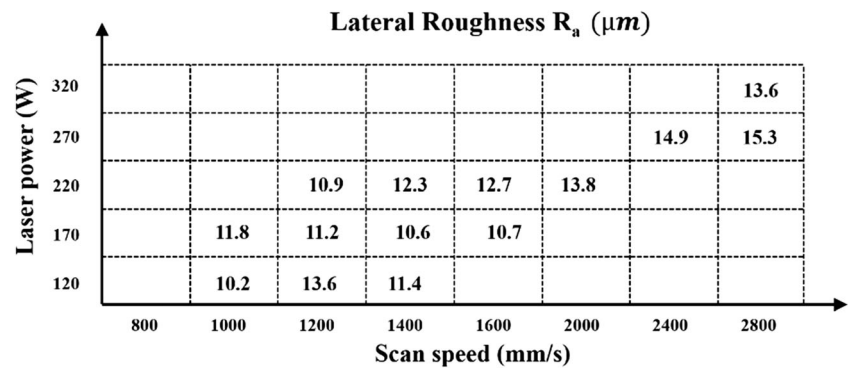


Fig. 11 Lateral surface roughness with scan speeds at 170 W of laser power



environment condition of the tests is close to the condition of the fill-scan mode, the stability of the process to fill a volume can be reasonably evaluated by the proposed method. In addition, the proposed method can provide more useful information such as the width of the single-line track and the lateral surface roughness, which would be helpful for determining optimal process parameters for the contour-scan in SLM process.

The proposed method can be used to build a stable process window for understanding the evolution of microstructures under controlled condition in a new material.

Acknowledgments I wish to thank Son yong and his team in Korea Institute of Industrial Technology (KITECH) for their help in the fabrication of specimens.

Funding information This research was supported by the Tongmyong University Research Grants 2017A002.

References

- Moon SK, Tan YE, Hwang JH, Yoon YJ (2015) Application of 3d printing technology for designing light-weight unmanned aerial vehicle wing structures. *Int J Precis Eng Manuf-GT* 1(3):223–228
- Das S, Wohler M, Beaman JJ, Bourell DL (1998) Producing metal parts with selective laser sintering/hot isostatic pressing. *JOM* 50(12):17–20
- Vandenbroucke B, Kruth JP (2007) Selective laser melting of bio-compatible metal for rapid manufacturing of medical parts. *Rapid Prototyp J* 13(4):196–203
- Lachmayer R, Kloppenburg G, Wolf AG (2015) Rapid prototyping of reflectors for vehicle lighting using laser activated remote. In *Light-emitting diodes: materials, devices, and applications for solid State Lighting XIX SPIE*: 938305
- Bean GE, Witkin DB, McLouth TD, Patel DN, Zaldivar RJ (2018) Effect of laser focus shift on surface quality and density of Inconel 718 parts produced via selective laser melting. *Addit Manuf* 22: 207–215
- Khorasani AM, Gibson I, Ghaderi AR (2018) Rheological characterization of process parameters influence on surface quality of Ti-6Al-4V parts manufactured by selective laser melting. *Int J Adv Manuf Technol* 97(9–12):3761–3775
- Ma CL, Gu DD, Dai DH, Du L, Zhng H (2018) Development of interfacial stress during selective laser melting of TiC reinforced TiAl composites: influence of geometric feature of reinforcement. *Mater Des* 157:1–11
- Jafari D, Wits WW (2018) The utilization of selective laser melting technology on heat transfer devices for thermal energy conversion applications: a review. *Renew Sust Energ Rev* 91:420–442
- Yap CY, Chua CK, Dong ZL, Liu ZH, Zhang DQ, Loh LE, Sing SL (2015) Review of selective laser melting: materials and applications. *Appl Phys Rev* 2(4):041101
- Shipley H, McDonnell D, Culleton M, Lupoi R, O'Donnell G, Trimble D (2018) Optimisation of process parameters to address fundamental challenges during selective laser melting of Ti-6Al-4V: a review. *Int J Mach Tool Manu* 128:1–20
- Clijsters S, Craeghs T, Bult S, Kempen K, Kruth JP (2014) In situ quality control of the selective laser melting process using a high-speed, real-time melt pool monitoring system. *Int J Adv Manuf Technol* 75(5–8):1089–1101
- Ahn IH, Moon SK, Hwang JH, Guijun B (2017) Characteristic length of the solidified melt pool in selective laser melting process. *Rapid Prototyp J* 23(2):370–381
- Kempen K, Thijs L, Van Humbeeck J, Kruth JP (2015) Processing AlSi10Mg by selective laser melting: parameter optimisation and material characterization. *Mater Sci Technol* 31(8):917–923
- Gong HJ, Rafi K, Starr T, Stucker B (2013) The effects of processing parameters on defect regularity in Ti-6Al-4V parts fabricated by selective laser melting and electron beam melting. *24th Annual International Solid Freeform Fabrication Symposium*, Aug, Austin, TX, USA, pp. 12–14
- Di W, Yang YQ, Su XB, Che YH (2011) Study on energy input and its influences on single-track, multi-track, and multi-layer in SLM. *Int J Adv Manuf Technol* 58(9–12):1189–1199
- Zhang DQ, Cai QH, Liu JH, He J, Li R (2012) Microstructural evolution and formation of selective laser melting W–Ni–Cu composite powder. *Int J Adv Manuf Technol* 67(9–12):2233–2242
- Song B, Dong SJ, Deng SH, Liao HL, Coddet C (2014) Microstructure and tensile properties of iron parts fabricated by selective laser melting. *Opt Laser Technol* 56:451–460
- Li R, Shi YS, Liu JH, Xie Z, Wang ZG (2009) Selective laser melting W–10 wt.% Cu composite powders. *Int J Adv Manuf Technol* 48(5–8):597–605
- Childs THC, Hauser C, Badrossamay M (2005) Selective laser sintering (melting) of stainless and tool steel powders: experiments and modelling. *Inst Mech Eng B* 219(4):339–357
- Khan M, Dicken P (2012) Selective laser melting (SLM) of gold (Au). *Rapid Prototyp J* 18(1):81–94
- King WE, Barth HD, Castillo VM, Gallegos GF, Gibbs JW, Hahn DE, Kamath C, Rubenchik AM (2014) Observation of keyhole-mode laser melting in laser powder-bed fusion additive manufacturing. *J Mater Process Technol* 214(12):2915–2925
- Spierings AB, Levy G (2009) Comparison of density of stainless steel 316L parts produced with selective laser melting using

- different powder grades. 19th Annual International Solid Freeform Fabrication Symposium, Aug, Austin, TX, USA pp. 342–353
23. Li R, Liu JH, Shi YS, Wang L, Jiang W (2011) Balling behavior of stainless steel and nickel powder during selective laser melting process. *Int J Adv Manuf Technol* 59(9–12):1025–1035
 24. Sun ZG, Tan XP, Tor SB, Yeong WY (2016) Selective laser melting of stainless steel 316L with low porosity and high build rates. *Mater Des* 104:197–204
 25. Yadroitsev I, Yadroitsava I, Bertrand P, Smurov I (2012) Factor analysis of selective laser melting process parameters and geometrical characteristics of synthesized single tracks. *Rapid Prototyp J* 18(3):201–208
 26. Yuan PP, Gu DD (2015) Molten pool behaviour and its physical mechanism during selective laser melting of TiC/AlSi10Mg nanocomposites: simulation and experiments. *J Phys D Appl Phys* 48(3):035303
 27. Fox JC, Moylan SP, Lane BM (2016) Effect of process parameters on the surface roughness of overhanging structures in laser powder bed fusion additive manufacturing. *Procedia CIRP* 45:131–134
 28. Jamshidinia M, Kovacevic R (2015) The influence of heat accumulation on the surface roughness in powder-bed additive manufacturing. *Surf Topogr* 3(1):014003

Publisher's note Springer Nature remains neutral with regard to jurisdictional claims in published maps and institutional affiliations.